Photoresponsive adenosine derivatives for optical control of adenosine A_{2A} receptor in living cells

Harufumi Suzuki[a‡], Tomohiro Doura*[a‡], Yuya Matsuba[a], Yuma Matsuoka[a], Tsuyoshi Araya[b], Hidetsugu Asada[b], So Iwata[b,c] and Shigeki Kiyonaka*[a,c]

[a]Department of Biomolecular Engineering, Graduate School of Engineering, Nagoya University, Nagoya 464-8603, Japan

[b]Department of Cell Biology, Graduate School of Medicine, Kyoto University, Kyoto 606-8501, Japan.

[c]RIKEN SPring-8 Center, Hyogo 679-5148, Japan.

[d]Institute of Nano-Life-Systems, Institutes of Innovation for Future Society, Nagoya University, Nagoya 464-8603, Japan.

*Correspondence: doura_t@chembio.nagoya-u.ac.jp
kiyonaka@chembio.nagoya-u.ac.jp

‡These authors contributed equally to this work.

Abstract

Subtype-selective ligands with photoswitchable properties are highly desired for photopharmacology of G protein-coupled receptors (GPCRs). We developed photoswitchable ligands targeting adenosine A_{2A} receptor ($A_{2A}R$), a GPCR subtype. Spatiotemporal activation of $A_{2A}R$ was successfully demonstrated in living cells using the photoswitchable ligand.

Main text

Optical control of proteins of interest (POIs) using photoresponsive ligands, known as photopharmacology, is powerful for elucidating cellular function with high spatiotemporal resolution in living cells and animals.[1] Photoresponsive ligands are mainly categorized into caged compounds or photoswitchable ligands. In caged compounds, the activity of ligands for POIs is temporarily masked with covalently bound photoremovable protecting groups.[2,3] Although the active species can be released through photo irradiation, the chemical process is irreversible. In contrast, photoswitchable ligands have photo-isomerizable groups, such as azobenzene, that covalently attach to target ligands. Reversible *trans*-to-*cis* or *cis*-to-*trans* isomerization of azobenzene can be induced by light of different wavelengths, allowing precise control of the function of POIs.[4,5] However, photoswitchable ligands are more challenging to design than caged compounds because structural changes in azobenzene must be strongly correlated with changes in the affinity for POIs. Indeed, the variety of available photoswitchable ligands targeting druggable proteins is still limited.[6–9]

G protein-coupled receptors (GPCRs) are the targets of 30% to 40% of current drugs. Approximately 850 GPCRs are encoded in the human genome, of which half are considered potential drug targets.[10] GPCRs can be classified into multiple groups according to the endogenous ligand, including acetylcholine, adenosine, dopamine, and serotonin. Typically, each group has several subtypes that are activated by the same endogenous ligand. For example, adenosine receptors are composed of four subtypes, namely A_1, A_{2A}, A_{2B}, and A_3,[11] of which A_1R and $A_{2A}R$ have high affinities for adenosine (in the range of 10^{-7} M).[12] $A_{2A}R$ is a Gs-coupled GPCR and is expressed in various tissues, such as spleen, thymus, leukocytes, blood platelets, olfactory bulb, and other brain regions.[13] Abnormality of $A_{2A}R$ causes diseases such as cancer and Parkinson's disease, which makes $A_{2A}R$ a potential drug target.[14,15] In contrast, A_1R is a Gi/o-coupled GPCR and plays various physiological roles in the body.[16] Thus, selective activation of $A_{2A}R$ with high spatiotemporal resolution would be powerful for elucidating the physiological and pathological roles of $A_{2A}R$ in tissues and animals.

Photoswitchable ligands targeting $A_{2A}R$ would be valuable tools for analyzing the physiological roles of $A_{2A}R$ with high spatiotemporal resolution. However, to date, there are no photoswitchable ligands exhibiting both adequate photoswitching properties and high selectivity for $A_{2A}R$. Therefore, we initiated the development of $A_{2A}R$-selective photoswitchable ligands applicable to living

mammalian cells (Fig. 1). To obtain photoswitchable ligands targeting $A_{2A}R$, a photoswitchable moiety was introduced to the 2- or 6-position of the purine of adenosine (Fig. 2a). Ethyl azobenzene (EtAB) or methyl azobenzene (MeAB) was introduced to the 2- or 6-position to obtain compounds **1**, **2**, **4**, and **5**. We also designed and synthesized compounds **3** and **6** with attached arylazopurine consisting of azophenyl (AzPh) group and the purine of adenosine (Fig. 2a, Scheme S1, ESI†).

To investigate the photophysical properties of the synthesized adenosine derivatives (**1**–**6**), ultraviolet–visible (UV–vis) absorption spectra of **1**–**6** were acquired at thermal equilibrium and in the photostationary state after irradiation with 365 nm light-emitting diode (LED) light (PSS_{365}). In the spectra of **1**–**5**, the absorbance peak at 320–360 nm, corresponding to the π–π* transition of the *trans*-isomer of azobenzene or 2-arylazopurine, decreased in intensity after 365 nm light irradiation (Fig. S1, ESI†). This spectral change indicated that **1**–**5** underwent *trans*-to-*cis* photoisomerization upon 365 nm light irradiation. In contrast, 365 nm light irradiation did not lead to changes in the spectra of **6** (Fig. S1, ESI†). This indicated that either photoisomerization of **6** did not occur or the reverse *cis*-to-*trans* transition occurred too rapidly to be detected. We also measured the UV–vis spectra of **1**–**6** in the photostationary state after irradiation with 470 nm LED light (PSS_{470}). The intensity of the π–π* transition peak of **1**–**5** increased, which indicated that 470 nm light irradiation induced the *cis*-to-*trans* photoisomerization of these compounds (Fig. S1, ESI†). To determine the proportions of *trans*- and *cis*-isomers produced after **1**–**5** were irradiated with 365 nm or 470 nm light, we acquired ^{1}H NMR spectra of these compounds in the PSS_{365} or PSS_{470} (Fig. S2, ESI†). As shown in Table S1 (ESI†), adenosine derivatives with an attached azobenzene group (**1**, **2**, **4**, **5**) preferentially transformed into the *cis*-isomer (80–94%) in the PSS_{365} and the *trans*-isomer (72–74%) in the PSS_{470}. Similarly, compound **3** with attached arylazopurine preferentially transformed into the *cis*-isomer (75%) in the PSS_{365} and the *trans*-isomer (60%) in the PSS_{470} (Fig. S2 and Table S1, ESI†).

Having obtained adenosine derivatives **1**–**5** with good photoswitching properties, we proceeded to investigate the photopharmacological properties of these compounds with respect to A_1R and $A_{2A}R$ using living mammalian cells. HEK293 cells were used to express A_1R or $A_{2A}R$ along with Gα15 protein,[17] and cellular responses were evaluated by monitoring changes in intracellular Ca^{2+} concentration using Cal-520, a fluorescent Ca^{2+} indicator. As shown in Fig. S3 (ESI†), adding adenosine to these cells increased the fluorescence of Cal-520 in a dose-dependent manner, indicating

that both A_1R and $A_{2A}R$ were functionally expressed in HEK293 cells. Then, Ca^{2+} responses were evaluated by adding each concentration of **1**–**5** before or after 365 nm light irradiation. As shown in Fig. S4 (ESI†), the *trans*-form or the PSS_{365} of **1**, **3**, **4**, and **5** in the range of 10–100 nM activated $A_{2A}R$. In contrast, **2** in the same concentration range failed to activate $A_{2A}R$, indicating that the length of the linker between purine and azobenzene was important in 2-position substituted adenosine derivatives. These assays revealed that the half-maximal effective concentration (EC_{50}) of **4** for activating $A_{2A}R$ differed by 13-fold between the *trans*-form and the PSS_{365} (Table 1). However, the ratio of EC_{50} for activating A_1R to that for activating $A_{2A}R$ (A_1/A_{2A} ratio) was 0.46, indicating that **4** had insufficient subtype selectivity, namely between $A_{2A}R$ and A_1R. In contrast, 2-position substituted **1** and **3** had high selectivity for activating $A_{2A}R$ (A_1/A_{2A} ratio > 52). The ratio of the EC_{50} of the *trans*-form to that of the PSS_{365} for activating $A_{2A}R$ (*trans*/365 ratio) was 3.1 and 0.08 for **1** and **3**, respectively (Table 1). This indicated that $A_{2A}R$ could be activated through the *trans*-to-*cis* photoconversion of **1** and the *cis*-to-*trans* photoconversion of **3**. Thus, we selected **1** and **3** as potentially effective $A_{2A}R$-selective photoswitchable ligands.

As described above, 365 nm light irradiation resulted in a 10-fold increase in the EC_{50} of **3** for activating $A_{2A}R$ (Table 1). Given that PSS_{365} comprised 25% of the *trans*-isomer of **3** (*trans*-**3**) (Fig. S2, ESI†), EC_{50} was determined in the presence of 25% of *trans*-**3** showing low EC_{50}. Importantly, the *cis*-isomer of **3** (*cis*-**3**) could be isolated using high-performance liquid chromatography (HPLC), which indicated that *cis*-**3** was relatively stable ($t_{1/2}$ = 40.7 h) in HEPES-buffered saline (HBS, pH 7.4) at 37 °C (Fig. S5, ESI†). Then, we evaluated the dose-dependency of activating $A_{2A}R$ by *cis*-**3**. As shown in Fig. 2b, the activity of *cis*-**3** against $A_{2A}R$ was low, and EC_{50} was greater than 1,000 nM (Table S2, ESI†). Of note, a short period of 470 nm light irradiation induced the *cis*-to-*trans* photoisomerization of *cis*-**3** (Fig. 2c), and low concentrations (10 nM range) of **3** in the PSS_{470} activated $A_{2A}R$ (Fig. 2b). Although isolation of the *cis*-isomer is required, **3** would be useful for the selective activation of $A_{2A}R$ with short-time blue light (470–490 nm) irradiation. Thus, we termed **3** as photoAd(blue).

Thermally stable isomers that can be induced to transform into the active species reversibly are ideal photoswitchable ligands. As described above, 365 nm light irradiation to thermally stable *trans*-form of **1** resulted in a 3.1-fold decrease in the EC_{50} for activating $A_{2A}R$ (Table 1). To improve the

difference between the EC_{50} of the *trans*-form and that of the PSS_{365} (*trans*/365 ratio) for activating $A_{2A}R$, we designed and synthesized **7**–**10** by introducing substituents to the azobenzene moiety of **1** (Fig. 3a, Scheme S3, ESI†). UV–vis and ^1H NMR spectra before and after 365 nm or 470 nm light irradiation indicated that **7**–**10** exhibited excellent photoswitching properties (Fig. S6 and S7, Table S1, ESI†). The pharmacological properties of **7**–**10** were evaluated using HEK293 cells expressing $A_{2A}R$. The results revealed that the EC_{50} of the *trans*-form of these compounds were dependent on the substituents of the azobenzene moiety (Table 1, Fig. S8, ESI†). In contrast, the EC_{50} of these compounds in the PSS_{365} were less affected by the substituents. These assays revealed that **10**, with a *tert*-butyl group at the *para* position of azobenzene, had the highest *trans*/365 ratio (Table 1, Fig. 3b). Similar to the case of **1**, high concentrations (μM range) of **10**, whether in the *trans*-form or PSS_{365}, failed to activate A_1R, indicating that **10** had sufficient selectivity for the $A_{2A}R$ subtype. In addition, photoisomerization of **10** between the *trans*- and *cis*-isomer was reversible and repeatable (Fig. 3c), and we termed **10** as photoAd(vio).

With the $A_{2A}R$-selective photoswitchable ligand, photoAd(vio) in hand, we next evaluated the spatiotemporal activation of $A_{2A}R$-expressing living cells with violet light irradiation. After adding Cal-520 to HEK293 cells expressing $A_{2A}R$ or A_1R, the *trans*-form of photoAd(vio) (100 nM) was added to the culture medium. A confocal microscope was utilized to monitor the fluorescence changes of the Ca^{2+} indicator before and after irradiation of violet (405 nm) laser to the regions of interest (ROIs) (Fig. 3d). As shown in Fig. S9 (ESI†), irradiation of violet (400 nm) LED light can induce *trans*-to-*cis* isomerization of photoAd(vio). In cells expressing $A_{2A}R$, the fluorescence of Cal-520 increased markedly in cells irradiated with 405 nm laser, but not in surrounding cells (Fig. 3d, e). In contrast, prominent fluorescence changes of Cal-520 were not observed in the absence of photoAd(vio), $A_{2A}R$ expression, or 405 nm laser irradiation (Fig. 3e), suggesting that the increase in fluorescence intensity was induced by the photoswitching of photoAd(vio). Consistent with the pharmacological properties of photoAd(vio), the fluorescence of Cal-520 did not change in cells expressing A_1R even after 405 nm laser irradiation (Fig. 3d, e). These results indicated that the combination of photoAd(vio) and violet light irradiation was effective in the activation of living cells expressing $A_{2A}R$ with high spatiotemporal resolution.

In conclusion, we developed photoAd(blue) and photoAd(vio) as $A_{2A}R$-selective photoresponsive ligands. To the best of our knowledge, two photoswitchable ligands for adenosine receptors have been developed by different groups.[18,19] However, both ligands exhibit insufficient subtype selectivity or pharmacological characterization. In this context, photoAd(vio) would be powerful as a highly selective photoswitchable ligand for $A_{2A}R$, in which the *cis*-isomer show lower EC_{50} for $A_{2A}R$. In contrast, in the case of photoAd(blue), the thermally stable *trans*-isomer showed lower EC_{50} for $A_{2A}R$. Of note, we successfully determined the X-ray crystal structure of $A_{2A}R$ with photoNECA(blue), an analogue of photoAd(blue).[20] Therefore, photoAd(blue) and its analogues would be powerful not only as photoresponsive ligands for photopharmacology but also as chemical probes for structural biology studies of $A_{2A}R$.

Conflicts of interest

The authors declare no competing financial interests.

Notes and references

1. M. Ricart-Ortega, J. Font and A. Llebaria, *Mol. Cell. Endocrinol.* 2019, **488**, 36−51.
2. G. C. R. Ellis-Davies, *Nat. Methods* 2007, **4**, 619–628.
3. T. Furuta and K. Noguchi, *Trends Anal. Chem.* 2004, **23**, 511–519.
4. W. A. Velema, W. Szymanski and B. L. Feringa, *J. Am. Chem. Soc.* 2014, **136**, 2178–2191.
5. A. A. Beharry and G. A. Woolley, *Chem. Soc. Rev.* 2011, **40**, 4422–4437.
6. M. Volgraf, P. Gorostiza, R. Numano, R. H. Kramer, E. Y. Isacoff and D. Trauner, *Nat. Chem. Biol.* 2006, **2**, 47−52.
7. A. Duran-Corbera, M. Faria, Y. Ma, E. Prats, A. Dias, J. Catena, K. L. Martinez, D. Raldua, A. Llebaria and X. Rovira, *Angew. Chem. Int. Ed.* 2022, **61**, e202203449.
8. S. Pittolo, X. Gómez-Santacana, K. Eckelt, X. Rovira, J. Dalton, C. Goudet, J.-P. Pin, A. Llobet, J. Giraldo, A. Llebaria and P. Gorostiza, *Nat. Chem. Biol.* 2014, **10**, 813−815.
9. N. N. Mafy, K. Matsuo, S. Hiruma, R. Uehara and N. Tamaoki, *J. Am. Chem. Soc.* 2020, **142**, 1763−1767.
10. T. Laeremans, Z. A. Sands, P. Claes, A. D. Blieck, S. D. Cesco, S. Triest, A. Busch, D. Felix, A. Kumar, V.-P. Jaakola and C. Menet, *Front. Mol. Biosci.* 2022, **9**, 863099.
11. P. A. Borea, S. Gessi, S. Merighi, F. Vincenzi and K. Varani, *Physiol. Rev.* 2018, **98**, 1591−1625.
12. A. van Waarde, R. A. J. O. Dierckx, X. Zhou, S. Khanapur, H. Tsukada, K. Ishiwata, G. Luurtsema, E. F. J. de Vries and P. H. Elsinga, *Med. Res. Rev.* 2018, **38**, 5−56.
13. M. de Lera Ruiz, Y.-H. Lim and J. Zheng, *J. Med. Chem.* 2014, **57**, 3623−3650.
14. M. T. Armentero, A. Pinna, S. Ferré, J. L. Lanciego, C. E. Müller and R. Franco, *Pharmacol. Ther.* 2011, **132**, 280–299.
15. A. Ohta, E. Gorelik, S. J. Prasad, F. Ronchese, D. Lukashev, M. K. K. Wong, X. Huang, S. Caldwell, K. Liu, P. Smith, J.-F. Chen, E. K. Jackson, S. Apasov, S. Abrams and M. Sitkovsky, *Proc. Natl. Acad. Sci. USA* 2006, **103**, 13132-13137.
16. S. Camandola, N. Plick and M. P. Mattson, *Neurochem. Res.* 2019, **44**, 214–227.

17. R. Kubota, W. Nomura, T. Iwasaka, K. Ojima, S. Kiyonaka and I. Hamachi, *ACS Cent. Sci.* 2018, **4**, 1211–1221.
18. M. I. Bahamonde, J. Taura, S. Paoletta, A. A. Gakh, S. Chakraborty, J. Hernando, V. Fernández-Dueñas, K. A. Jacobson, P. Gorostiza and F. Ciruela, *Bioconjugate Chem.* 2014, **25**, 1847−1854.
19. K. Hüll, V. Fernández-Dueñas, M. Schönberger, M. lópez-Cano, D. Trauner and F. Ciruela, *Bioconjugate Chem.* 2021, **32**, 1979−1983.
20. T. Araya, Y. Matsuba, H. Suzuki, T. Doura, N. Nuemket, E. Nango, M. Yamamoto, D. Im, H. Asada, S. Kiyonaka and S. Iwata, manuscript in preparation.

ORCID

Shigeki Kiyonaka: 0000-0002-4100-6738

Tomohiro Doura: 0000-0003-1826-6010

Tsuyoshi Araya: 0000-0002-7197-1053

Hidetsugu Asada: 0000-0001-6255-4728

So Iwata: 0000-0003-1735-2937

ACKNOWLEDGEMENTS

This work was funded by Grant-in-Aid for Scientific Research (KAKENHI) (Grant Number 19K16325 and 22K05351 to T.D., 19H05778 and 20H02877 to S.K.), and supported by JST ERATO Hamachi Innovative Molecular Technology for Neuroscience Project (Grant Number JPMJER1802 to S.K.). We thank Edanz (https://jp.edanz.com/ac) for editing a draft of this manuscript.

Table 1. Photopharmacological properties of **1**–**10** for $A_{2A}R$ and A_1R.

	EC_{50} for $A_{2A}R$ (nM)		*trans*/365 ratio [#1]	EC_{50} for A_1R (nM)		A_1/A_{2A} ratio [#2]
	trans	PSS_{365}		*trans*	PSS_{365}	
1	20 ± 7.1	6.4 ± 0.64	3.1	> 10000	> 10000	> 310
2	> 10000	> 10000	-	> 10000	> 10000	–
3, photoAd(blue)	19 ± 4.2	250 ± 110	0.08	> 1000	> 1000	> 52
4	1300 ± 290	99 ± 18	13	600 ± 64	220 ± 500	0.46
5	730 ± 920	610 ± 110	1.2	190 ± 14	430 ± 68	0.26
7	46 ± 8.7	21 ± 5.7	2.2	> 10000	> 10000	> 220
8	130 ± 13	41 ± 9.7	3.2	> 10000	> 10000	> 77
9	75 ± 6.7	17 ± 7.0	4.4	> 10000	> 10000	> 130
10, photoAd(vio)	860 ± 93	40 ± 7.4	22	> 10000	> 10000	> 12

#1; ratio of EC_{50} value between *trans*-form and PSS_{365} for $A_{2A}R$

#2; ratio of EC_{50} value for A_1R and $A_{2A}R$

FIGURES

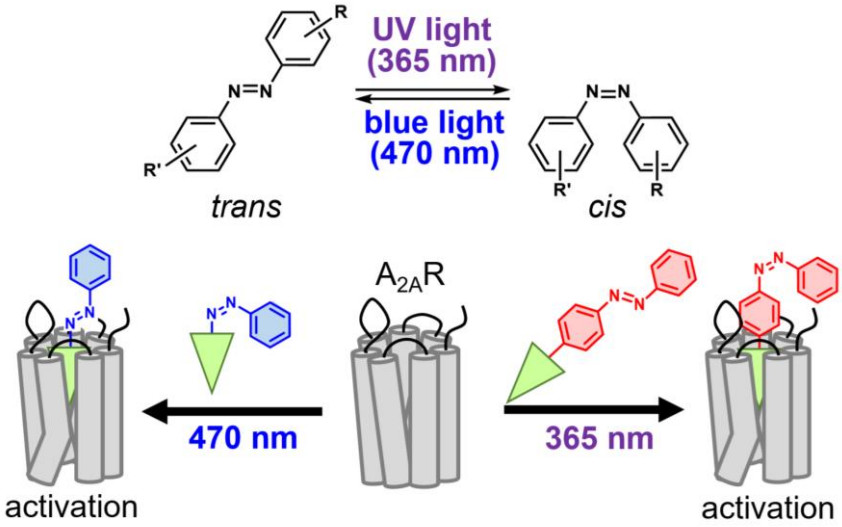

Fig 1. Schematic illustration of optical control of $A_{2A}R$ activity using photoswitchable adenosine derivatives.

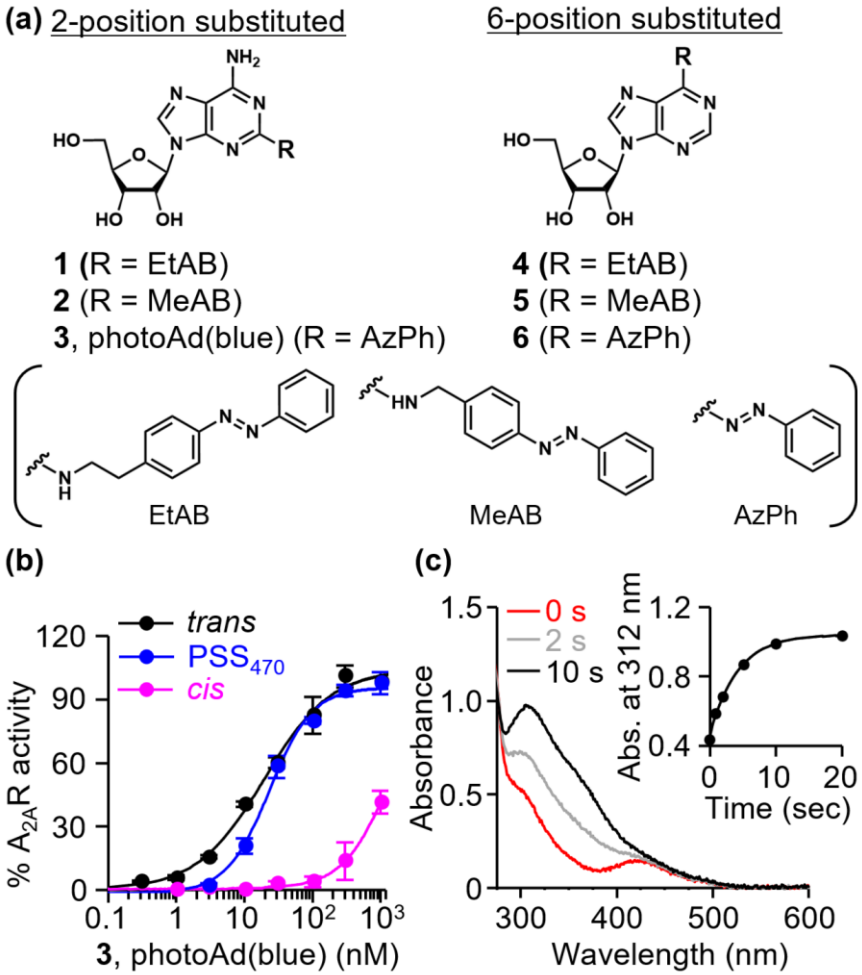

Fig 2. Development of an A_{2A}R-selective blue light-activatable ligand. (a) Chemical structures of compounds **1**–**6**. (b) Activity of *trans*-**3** (black), *cis*-**3** (magenta), and **3** in the PSS_{470} (blue) for A_{2A}R. Percentage of A_{2A}R activity was determined using the value activated by 1 μM adenosine as 100% (*N* = 3). Error bars indicate standard error of the mean (SEM). (c) Photoisomerization of *cis*-**3** was determined by UV-vis absorption spectra. The spectra of *cis*-**3** (10 μM) in HBS were measured after irradiation with 470 nm light (15 mW) in each period. The change of absorbance (Abs.) at 312 nm was shown in the inset.

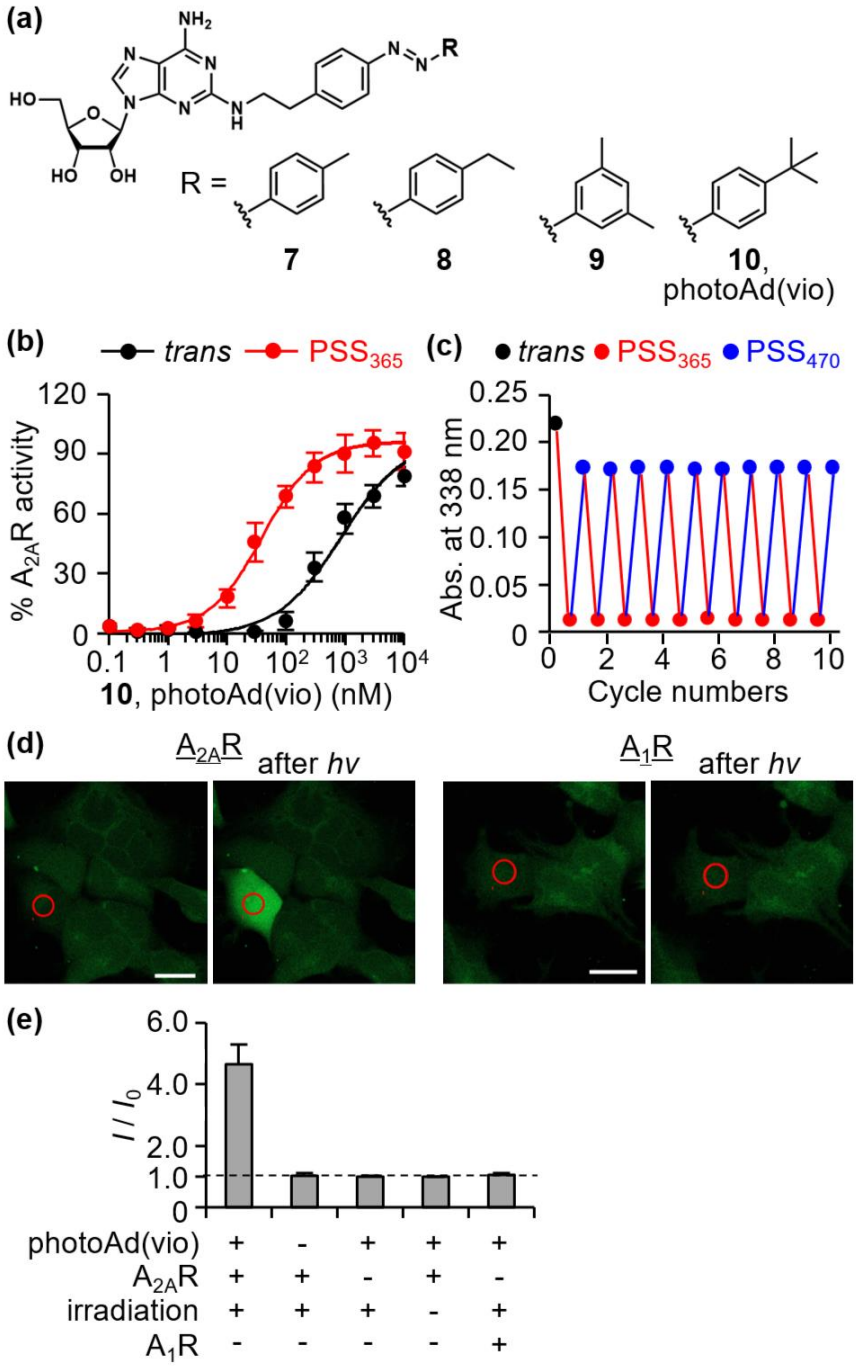

Fig 3. Development of an $A_{2A}R$ selective photoswitchable ligand. (a) Chemical structures of compounds **7**–**10**. (b) Activity of *trans*-**10** (black) and **10** in the PSS_{365} (red) for $A_{2A}R$ (N = 3). Error bars indicate SEM. (c) The change of absorbance at a maximum absorption wavelength (λ_{max}) of 338 nm for **10** (10 μM) in HBS after ten cycles of consecutive 365 nm light irradiation (red line) and 470 nm light irradiation (blue line). (d) Photoactivation of HEK293 cells expressing $A_{2A}R$ (left) or A_1R (right) with *trans*-**10** by 405 nm laser irradiation. ROIs shown in red were irradiated with 405 nm laser (*hv*). The scale bars show 20 μm. (e) Quantification of signal intensity of Cal-520 (N = 6–20). I_0 and I indicate maximum fluorescence intensity of the cells before and after laser irradiation, respectively. Data are presented as mean ± SEM.